Electromigration-Based Investigation of Corrosion Behaviour in Ternary Blended Reinforced Concrete

Kazi Naimul Hoque [1,*] and Francisco Presuel-Moreno [2]

[1] Department of Naval Architecture and Marine Engineering, Bangladesh University of Engineering and Technology (BUET), Dhaka, Bangladesh

[2] Department of Ocean and Mechanical Engineering, Florida Atlantic University (FAU), Dania Beach, Florida, USA

Email: kazinaim@name.buet.ac.bd (K.N.H.); fpresuel@fau.edu (F.P.M.)

*Corresponding author

***Abstract*—Two distinct sets of concrete mixes were prepared. In one mix, labeled T1, 20% of the cement was replaced with fly ash and 50% with slag. In the other mix, known as T2, 20% of the cement was substituted with fly ash and 8% with silica fume. The specimens were reinforced with three rebars and had a concrete cover of 2.5 cm. Various-sized reservoirs, ranging from 2.5 cm to 10 cm, were affixed to the top surface of the specimens, each filled with a 10% NaCl solution by weight. Electromigration method was employed, which accelerated chloride transport and lasted for a week to a few months. The influence of rebar length under the reservoir for two different ternary blended concrete mixes were investigated. This study describes corrosion behavior of reinforced concrete specimens via rebar potential measurements, linear polarization resistance and electrochemical impedance spectroscopy measurements. The evolution of rebar potential, solution resistance, polarization resistance, and corrosion current values were monitored for around 950 days. The experimental findings indicated that T1 concrete mixes exhibited larger corrosion current values in comparison to T2 concrete mixes for similar reservoir lengths.**

***Keywords*—reservoir lengths, slag, fly ash. silica fume, electromigration, corrosion current**

I. Introduction

The primary cause of concrete-reinforced structures (RC) deterioration in marine and high humidity environments is the corrosion of steel reinforcement. Neglecting this issue accelerates RC degradation, resulting in negative consequences like a reduced service life and decreased cross-sectional area of steel components. In RC structures, chloride-induced corrosion progresses slowly, posing challenges for timely decision-making information. The lack of research and data on corrosion initiation and progression complicates the problem, with studies indicating that substantial damage takes time to manifest [1–3]. Previous research [4, 5] indicates that incorporating cement substitutes like fly ash, silica fume, and blast-furnace slag can significantly reduce the risk of steel corrosion and enhance concrete impermeability. Silica fume improves durability, while fly ash and blast-furnace slag are preferred for workability and cost-effectiveness. Torii [6] noted that concrete with 50% Ground Granulated Blast-furnace Slag (GGBS) showed concrete resistance similar to 10% silica fume. Using these materials in finely granulated and hydrated forms can partially fill concrete pores, reducing chloride ion diffusion and substance permeation, thereby decreasing pore size, and increasing concrete resistance to deterioration.

In this research, two unique ternary blended concrete mixes were prepared. The anode's length was adjusted by customizing the solution reservoir dimensions. To expedite chloride ion ingress, the electromigration method was employed based on insights from prior studies [7–9]. Typically, rebar corrosion initiation occurs within weeks to a month. Measurements using Electrochemical Impedance Spectroscopy (EIS) and Linear Polarization Resistance (LPR) techniques were conducted to observe corrosion propagation. Key parameters, including rebar potential, solution resistance, polarization resistance, and corrosion current, were periodically monitored over approximately 950 days.

II. Experimental Details

A. Materials and Specimen Preparation

Two concrete mixes, labelled T1 and T2, were prepared. T1 consisted of 20% fly ash and 50% slag as cement replacements, while T2 incorporated 20% fly ash and 8% silica fume. Detailed information about these mixes is available in Table I, and specific mix specifications can be found in Appendix 2 of reference [10].

The rebar segments were carefully sized and wire-brushed for proper preparation. Additionally, a hexane solution was applied to cleanse the reinforcement thoroughly, removing any grease or impurities before the

Manuscript received January 8, 2024; revised February 2, 2024; accepted February 25, 2024; published September 25, 2024.

casting phase. Specimens in this study were sized at 30.5 cm × 30.5 cm × 7.6 cm (12 inches × 12 inches × 3 inches), each featuring three rebar sections with a 0.63 cm radius. Four specimens were prepared for each concrete mix (T1 and T2), all with a 2.5 cm concrete cover thickness. To enable electrical contact for corrosion monitoring, necessary drilling and tapping were conducted on each rebar.

TABLE I. CONCRETE MIX DETAIL FOR T1 AND T2 SPECIMENS

Mix	Cementitious Content	Cement Content	20% FA	8% SF	50% Slag	Fine agg.	Coarse agg.	w/cm ratio
	(kg/m^3)	(kg/m^3)	(kg/m^3)	(kg/m^3)	(kg/m^3)	(kg/m^3)	(kg/m^3)	
T1	390	117.5	78.3	0	195.2	761	1009	0.41
T2	390	289	70	31	0	790	1046	0.37

During casting, all specimens were embedded with either stainless steel mesh or a Titanium Mixed Metal Oxide (TiMMO) mesh on the top surface, later serving as the bottom surface during the experiment. These meshes, positioned at the centre of the rebar, had lengths ranging from 2.5 cm to 10 cm and a width of approximately 3 cm, aiming to expedite chloride transport. After one day, the melds containing the specimens were removed and placed in a fog room for curing. Following the casting process, the samples were initially stored in a highly humid environment at the State Materials Office (SMO) of the Florida Department of Transportation (FDOT) for approximately one month. Subsequently, these samples were relocated to the FAU-SeaTech campus, marking the next phase of the experiment. Initially, the samples were placed in a high humidity chamber at FAU-SeaTech, awaiting the setup of the solution reservoir. Once the solution reservoir was established, the samples were transferred to a laboratory environment with a relative humidity of 65% and a temperature of 21°C. A plastic reservoir was securely affixed to the top surface of each sample using marine adhesives. The reservoir was then filled with a 10% NaCl solution with the aim of initiating corrosion in various lengths of the rebar. Furthermore, a section of each concrete specimen, approximately one cm in size, was treated with a saturated calcium hydroxide solution. This step was taken to minimize the leaching of chemicals from the concrete by placing the samples on top of a white plastic mesh.

B. Electromigration

A power source was utilized to generate an electric field between the top and bottom meshes of each specimen, thereby establishing a potential difference. This was done with the intention of propelling the chlorides from the solution above the rebar into the concrete, guiding them toward the embedded rebar. The negative terminal of the power source was connected to the electrode submerged in the NaCl solution reservoir, while the positive terminal was connected to the embedded mesh in each specimen. Fig. 1 shows a visual depiction of the electromigration experimental arrangement. The electromigration technique was applied to each specimen. Initially, a 9 V applied potential was used. As the rebar potential was monitored relative to a Saturated Calomel Reference Electrode (SCE) while the electric field was active, a potential exceeding +2 V was noted. After 7 days, the applied voltage was decreased to 3 V. To determine the current magnitude when a specific voltage was applied over several days, the change in potential across a 100-ohm resistor was utilized. When the system was deactivated, the rebar potential was measured in reference to an SCE. Although not physically connected, the rebars underwent polarization because of the ionic current driven by the applied electric field. To ascertain the occurrence of corrosion, the rebar potential was continuously monitored for a specific period, often extending up to two hours, after disconnecting the system. If the most recent rebar potential measurement indicated the absence of corrosion, the applied potential was reinstated. The electromigration process persisted until an off-rebar potential, signifying a value of −0.150 Vsce or even more negative, was recorded. Previous research has demonstrated that corrosion typically initiates at a potential of −0.150 Vsce (−0.220 V vs. CSE) [7].

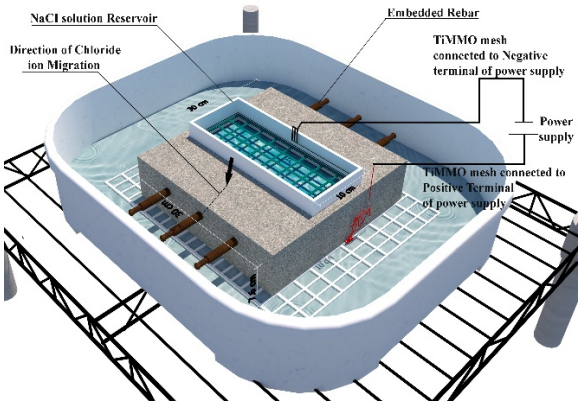

Fig. 1. Experimental setup used for electromigration.

TABLE II. DIFFERENT THREE REBAR SAMPLES MADE WITH T1 OR T2 MIXES

Sample Name	Reservoir Length (cm)	Migration Time Started	Migration Ending Date	Total Ampere-Hour
T1(25X)	5	10/31/2016	12/9/2016	0.40
T1(26X)	2.5	10/31/2016	11/11/2016	0.81
T1(27X)	10	10/31/2016	11/11/2016	0.81
T1(28X)	5	10/31/2016	11/11/2016	0.81
T2(29X)	10	10/31/2016	12/9/2016	0.51
T2(30X)	2.5	10/31/2016	12/9/2016	0.30
T2(31X)	5	11/1/2016	12/9/2016	0.46
T2(32X)	5	10/31/2016	11/11/2016	0.81

Table II presents the assigned labels for each sample, offering crucial information including the sample name/ID, reservoir length, and the duration of electromigration. Additionally, the table features a column that shows the

calculated Ampere-hour applied, which represents the accumulated values. It's important to note that during the initial phase of the experiment, each specimen underwent multiple electromigration periods.

III. Electrochemical Measurements

During the corrosion propagation phase, the rebar's Open-Circuit Potential (OCP) was routinely monitored using a SCE [11]. Measurements of solution resistance (Rs) and polarization resistance (Rc) were performed at least two days after disconnecting the system. The Rc value was determined by subtracting the solution resistance from the apparent polarization resistance. The EIS test covered a frequency range from 10 kHz to 1 Hz, with an impedance magnitude set at 54.51 Hz for Rs [12]. This procedure was conducted prior to the LPR measurement [12]. The LPR test ranged from 10 mV below the OCP to 1 mV above it. After approximately six months, LPR measurements were carried out from 8 mV below the OCP to the OCP, using a scan rate of either 0.1 mV/s or 0.05 mV/s.

During the period of electromigration, rebar potential measurements, EIS, and LPR tests were conducted. These measurements were performed only after the system had remained inactive for a minimum of two days. After terminating the electromigration process, these measurements were conducted monthly. Rc values obtained from LPR/EIS readings were converted to corrosion current (Icorr), by using the Stern-Geary equation, specifically, Icorr = B/Rp, where Rp represents the polarization resistance (previously defined as Rc), and B denotes the Stern-Geary coefficient. The value of B varied from 13 to 52 mV based on the corrosion condition of the steel, such as passive or active states [13, 14]. For this study, a value of 26 mV was used.

IV. Results and Discussion

In Fig. 2 and Fig. 3, the term "Day zero" represents the day at which the solution was introduced into the solution reservoir. It's important to note that this designation doesn't convey the specimen's age. Fig. 2 and Fig. 3 serves to visually depict the propagation of corrosion, which is portrayed on the right side of the dashed line. The arrow symbols that follow the dashed lines, situated to the right of them, indicate the post-migration period. This time frame marks the duration after the completion of the migration process. In cases where two black dashed lines are present, the space between them signifies the overall duration for which the samples were exposed to electromigration. Within this interval, the blue prisms represent the precisely measured timeframe during which the electric field was applied, also referred to as the "system on" period.

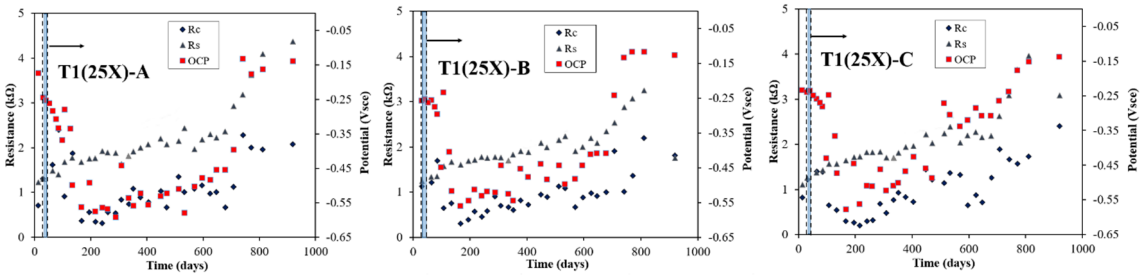

Fig. 2. Rs, Rc, and rebar potential measured on selected T1 sample (25X) under 5 cm reservoir.

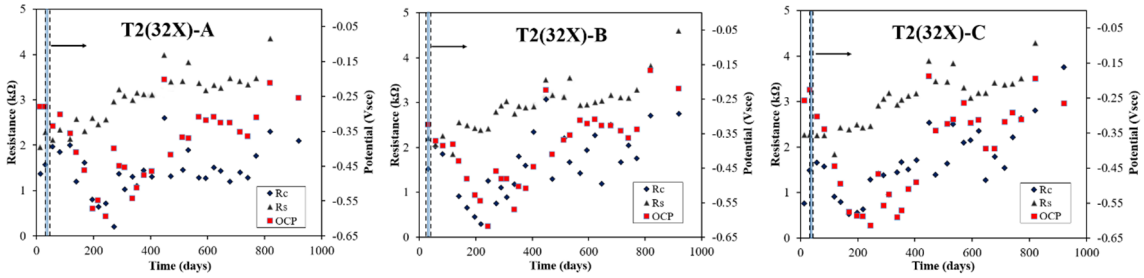

Fig. 3. Rs, Rc, and rebar potential measured on selected T2 sample (32X) under 5 cm reservoir.

Fig. 2 visually presents the evolution of rebar potential, Rs, and Rc for three specific rebars within the T1 sample (25X), identified as 25X-A, 25X-B, and 25X-C. The T1 sample utilized a solution reservoir with a size of 5 cm. Interestingly, all these rebars exhibited negative potential values and lower Rc values in a relatively short period of approximately 40 days during the electromigration. In the case of 25X-A rebar, the rebar potential witnessed a significant decline after electromigration ceased, reaching a value of -0.592 Vsce by day 288. Subsequently, the rebar potential gradually shifted towards more positive values. Over this period, Rs values exhibited a consistent upward trend, while Rc values remained below 2 k□ throughout the monitoring period for 25X-A rebar. For 25X-B rebar, the rebar potential experienced a sharp drop following the removal of electromigration, reaching −0.545 Vsce by day 195. The rebar potential then displayed fluctuations until day 750, therefore trending towards more positive values. Similar to 25X-A, Rs values increased steadily, while Rc values exhibited fluctuations and generally remained below 1.5 k□ during most of the monitoring period for 25X-B rebar. Examining 25X-C rebar, it's evident that the

rebar potential significantly decreased after the discontinuation of electromigration, reaching −0.579 Vsce by day 167. Subsequently, the rebar potential gradually drifted towards more positive values over time. In this case as well, Rs values displayed a continuous upward trend, while Rc values exhibited fluctuations for most of the monitoring period for 25X-C rebar. By day 534, rebar potential values were measured as follows: −0.581 Vsce for 25X-A, −0.499 Vsce for 25X-B, and −0.306 Vsce for 25X-C. These measurements underscore the variations in rebar potential, Rs, and Rc values among the different rebars over the given duration. Similar findings on rebar potential, Rs, and Rc values were observed in these studies [15–18].

Fig. 3 offers a visual representation of three distinct plots illustrating the dynamic changes in rebar potential, Rs, and Rc for three specific rebars within the T2 sample (32X), denoted as 32X-A, 32X-B, and 32X-C. The T2 sample employed a 5 cm-sized solution reservoir. Notably, all these rebars exhibited negative potential values and lower Rc values within a relatively brief period, approximately 12 days, during the electromigration process. In the case of 32X-A rebar, after electromigration ceased, the rebar potential underwent a notable decline, reaching −0.594 Vsce by day 244. Subsequently, the rebar potential displayed fluctuations and gradually shifted towards more positive values over time. Rs values demonstrated a consistent upward trajectory, while Rc values exhibited a fluctuating pattern throughout the monitoring period for 32X-A rebar. Regarding 32X-B rebar, the rebar potential experienced a sharp decrease following the discontinuation of electromigration, reaching −0.620 Vsce by day 244. The rebar potential then trended towards more positive values as the days progressed. Both Rs and Rc values displayed fluctuating patterns for most of the monitoring period for 32X-B rebar. Observing 32X-C rebar, it's evident that the rebar potential significantly decreased after the removal of electromigration, reaching −0.619 Vsce by day 244. Therefore, the rebar potential exhibited fluctuations and gradually drifted towards more positive values over time. Rs values showed a consistent increase, while Rc values displayed a fluctuating pattern for most of the monitoring period for 32X-C rebar. On day 513, rebar potential values were recorded as follows: −0.367 Vsce for 32X-A, −0.369 Vsce for 32X-B, and −0.323 Vsce for 32X-C. These measurements highlight the disparities in rebar potential, Rs, and Rc values across the distinct rebars during the specified timeframe. The results for the other T1 and T2 three rebar specimens can be found in references [10, 19–21].

Table III provides the average values of Rs, Rc, and rebar potential, as determined from LPR/EIS measurements conducted on three rebar specimens T1 and T2. These averages were computed based on data collected over an approximately 950-day monitoring period. In the case of T1 specimens, it was observed that rebar segments embedded in specimens with smaller solution reservoir sizes (2.5 cm and 5 cm) exhibited the highest average Rs and Rc values. Conversely, rebar segments within specimens featuring a larger solution reservoir size (10 cm) displayed the lowest average Rs and Rc values. For the T2 specimens, it was noted that rebar segments embedded in specimens with a smaller solution reservoir size (2.5 cm) had the highest average Rs and Rc values. On the other hand, rebar segments within specimens with a larger solution reservoir size (10 cm) exhibited the lowest average Rs and Rc values. Across all the specimens, the average rebar potential values consistently measured were more negative than −0.150 Vsce. Notably, for rebar segments embedded in T1 (25X-A) specimens with 5 cm reservoir length and T2 (29X-A) specimens with 10 cm reservoir length, the average rebar potential values were even more negative, dipping below −0.425 Vsce. It's crucial to emphasize that the position of the rebar within the concrete, as well as its proximity to the solution reservoir, had a significant impact on the measured rebar potential and other recorded data. In specific instances, excessive moisture content led to corrosion of the rebar exposed to the air, likely affecting the monitored Rc values and the measured rebar potential.

TABLE III. AVERAGE: RS, RC, AND REBAR POTENTIAL OBTAINED FROM LPR/EIS READINGS

Sample Name	Reservoir Length (cm)	Rebar Number	Average values obtained from LPR/EIS		
			Rs (k□)	Rc (k□)	Rebar potential (Vsce)
T1(25X)	5	A	2.17	1.10	−0.429
		B	1.97	0.96	−0.398
		C	2.07	1.00	−0.364
T1(26X)	2.5	A	2.93	1.41	−0.383
		B	2.57	1.45	−0.364
		C	2.74	1.37	−0.251
T1(27X)	10	A	1.61	0.95	−0.385
		B	1.59	0.93	−0.370
		C	1.81	1.06	−0.330
T1(28X)	5	A	2.79	2.07	−0.201
		B	2.51	1.98	−0.180
		C	2.79	2.34	−0.199
T2(29X)	10	A	2.25	0.96	−0.463
		B	2.15	1.22	−0.300
		C	2.24	1.43	−0.264
T2(30X)	2.5	A	4.38	1.91	−0.242
		B	3.84	2.43	−0.234
		C	4.58	2.27	−0.257
T2(31X)	5	A	3.10	1.39	−0.303
		B	2.91	1.64	−0.281
		C	3.10	2.46	−0.261
T2(32X)	5	A	3.10	1.43	−0.383
		B	2.91	1.83	−0.396
		C	3.06	1.64	−0.399

Variations in corrosion potential, observed in reinforced concrete samples, arise from differing levels of corrosion activity within distinct regions. These fluctuations are subject to a variety of influencing factors, including disparities in concrete compositions, the presence of oxygen, moisture content, and chloride concentration. These elements collectively give rise to localized corrosion, resulting in potential fluctuations. Moreover, shifts in the corrosion environment can also lead to

changes in corrosion potential. Factors such as temperature and humidity play a significant role in shaping the electrochemical reactions occurring at the steel reinforcement, thus causing potential variations. These fluctuations become evident as environmental conditions impact the pace of corrosion reactions and modify the electrochemical behaviour of the system. Consequently, the observed potential fluctuations are indicative of the dynamic nature of the corrosion process, influenced by these environmental factors.

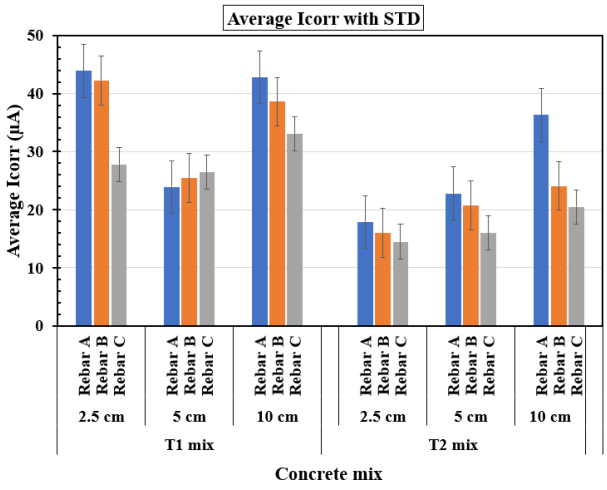

Fig. 4. Variation of average Icorr with length of solution reservoir for T1 and T2 concrete mixes cast with three rebar.

Fig. 4 provides a summary of the correlation between the average Icorr and the length of the solution reservoir for T1 and T2 concrete mixes. These average Icorr values were determined using the LPR/EIS method and were based on data collected over an approximately 950-day monitoring period.

The impact of different ternary blended concrete mixes (T1 and T2) on corrosion behavior involves intricate chemical and physical interactions within the concrete matrix. T1 and T2 mixes incorporate cement substitutes like fly ash, slag, and silica fume. These materials chemically interact with the concrete matrix, influencing corrosion behavior. For example, slag and fly ash can bind chloride ions, reducing their availability for steel corrosion. Silica fume's reactivity enhances concrete durability. The addition of cement substitutes alters the pore structure and permeability of the concrete. Finely granulated materials like fly ash and slag fill voids, reducing permeability. This affects the diffusion of corrosive agents, such as chlorides, and contributes to variations in corrosion current values. The alkaline environment generated by cementitious materials plays a crucial role in passivating the steel reinforcement. T1 and T2 mixes may differ in alkalinity, influencing the formation of a protective oxide layer on the steel surface. Variations in this passivation process impact corrosion potential and corrosion current values. Electrochemical reactions at the steel-concrete interface are affected by the composition of T1 and T2 mixes. The presence of different cementitious materials alters the kinetics of these reactions, influencing parameters like corrosion potential and corrosion current.

Therefore, the observed variations in corrosion behavior between T1 and T2 mixes result from a combination of chemical interactions involving cement substitutes, changes in pore structure, alkalinity-driven passivation, alterations in electrochemical reactions, chloride ion binding, microstructural modifications, and the interplay with reservoir lengths.

The relatively rapid onset of corrosion after discontinuing the electromigration process can be influenced by several factors, including specific characteristics of the concrete mix. During the electromigration process, chloride ions are actively driven into the concrete, accelerating their penetration. After discontinuing electromigration, the chloride ions present in the concrete continue to promote corrosion, leading to a rapid onset. The concentration of chloride ions, which can vary based on the concrete mix, is a crucial factor. Concrete's moisture content plays a significant role in the corrosion process. Excessive moisture can create a conducive environment for electrochemical reactions, facilitating the corrosion of steel reinforcement. Unique mix characteristics, such as the porosity of the concrete, can affect moisture retention and, consequently, the corrosion rate. The electrochemical conditions within the concrete, influenced by factors like pH and the presence of other ions, can impact the corrosion rate. Variations in the concrete mix may result in different electrochemical environments that affect the steel's susceptibility to corrosion. The type and proportion of cementitious materials (e.g., fly ash, silica fume, slag) in the concrete mix can influence its resistance to corrosion.

Furthermore, the lower corrosion current values in T2 concrete mixes (in comparison to T1 concrete mixes), achieved through the incorporation of fly ash and silica fume, indicate a concrete composition with improved corrosion resistance, reduced permeability, optimized pore structure, and chemical inhibition of corrosion. These characteristics collectively contribute to the overall durability and extended service life of concrete structures, making them more resilient to environmental challenges and reducing the economic burden of maintenance.

V. Conclusion

In this research, an electromigration technique was utilized to explore the corrosion characteristics of reinforced concrete specimens. It was observed that corrosion initiation occurred in all specimens just a few weeks after the discontinuation of the electromigration process. Subsequently, the propagation of corrosion was observed for roughly 950 days. Remarkably, the length of the solution reservoirs had a substantial impact on the corrosion-related parameters (solution resistance, polarization resistance, and rebar potential) derived from the electrochemical experiments.

Concerning the rebars integrated into T2 concrete mixes, there was a noticeable trend in which the corrosion current values increased as the length of the solution reservoir increased. However, it's important to note that an exception to this pattern was observed for the rebars embedded in T1 concrete mixes. When specimens with

similar reservoir lengths were compared, it became apparent that, in general, the corrosion current values were greater for the T1 specimens when contrasted with their T2 counterparts. This observation indicates that specimens prepared using T2 concrete mixes exhibit enhanced corrosion resistance and, therefore, greater durability when compared to those prepared with T1 concrete mixes.

CONFLICT OF INTEREST

The authors declare no conflict of interest.

AUTHOR CONTRIBUTIONS

Kazi Naimul Hoque worked on conceptualization, methodology, resources, data curation, writing-original draft preparation, visualization, investigation, writing-reviewing and editing; Francisco Presuel-Moreno worked on conceptualization, methodology, writing-reviewing and editing, supervision; all authors had approved the final version.

FUNDING

This research is funded through grants provided by Florida Atlantic University, as well as the National Center for Transportation Infrastructure Durability & Life-Extension (TriDurLE), and the Florida Department of Transportation (FDOT).

ACKNOWLEDGEMENT

The authors would like to express their gratitude to the Florida Department of Transportation (FDOT) for their assistance in preparing the samples. The opinions expressed in this paper are those of the authors and not necessarily those of FAU, the FDOT, and TriDurLE. Additionally, gratitude is expressed to the "Basic Research Grant" funded by BUET, for providing financial support to enhance the research endeavours.

REFERENCES

[1] M. Otieno, H. Beushausen, and M. Alexander, "Chloride-induced corrosion of steel in cracked concrete-part I: Experimental studies under accelerated and natural marine environments," *Cem. Concr. Res.*, vol. 79, pp. 373–385, 2016.

[2] M. Harilal, D. K. Kamde, S. Uthaman, R. P. George, R. G. Pillai, J. Philip, and S. K. Albert, "The chloride-induced corrosion of a fly ash concrete with nanoparticles and corrosion inhibitor," *Construction and Building Materials*, vol. 274, 122097, 2021.

[3] M. Harilal, R. P. George, S. K. Albert, and J. Philip, "A new ternary composite steel rebar coating for enhanced corrosion resistance in chloride environment," *Construction and Building Materials*, vol. 320, 126307, 2022.

[4] E. F. Irassar, M. Gonzalez, and V. Rahhal, "Sulphate resistance of type V cements with limestone filler and natural pozzolana," *Cem. Concr. Compos.*, vol. 22, pp. 361–368, 2000.

[5] K. M. A. Hossain and M. Lachemi, "Corrosion resistance and chloride diffusivity of volcanic ash blended cement mortar," *Cem. Concr. Res*., vol. 34, no. 4, pp. 695–702, 2004.

[6] K. Torii, T. Sasatani, and M. Kawamura, "Effects of fly ash, blast furnace slag, and silica fume on resistance of mortar to calcium chloride attack," in *Proc. Fifth International Conference on Fly Ash, Silica Fume, Slag, and Natural Pozzolans in Concrete*, American Concrete Institute, SP-153, vol. 2, 1995, pp. 931–949.

[7] F. Presuel-Moreno, H. Balasubramanian, and Y. Y. Wu, "Corrosion of reinforced concrete pipes: an accelerated approach," *Corrosion 2013*, paper no. C2013-0002551, Houston, TX: NACE, 2013.

[8] K. N. Hoque, F. Presuel-Moreno, and M. Nazim, "Corrosion of carbon steel rebar in binary blended concrete with accelerated chloride transport," *J. Infrastruct. Preserv. Resil.*, vol. 4, no. 26, 2023. https://doi.org/10.1186/s43065-023-00092-7

[9] K. N. Hoque, F. Presuel-Moreno, and M. Nazim, "Accelerated electromigration approach to evaluate chloride-induced corrosion of steel rebar embedded in concrete," *Advances in Materials Science and Engineering*, vol. 2023, 2023. https://doi.org/10.1155/2023/6686519

[10] F. Presuel-Moreno, M. Nazim, F. Tang, K. Hoque, and R. Bencosme, "Corrosion propagation of carbon steel rebars in high performance concrete," BDV27-977-08 Final Report for FDOT, 2018.

[11] ASTM C876-09, "Standard test method for corrosion potentials of uncoated reinforcing steel in concrete," *Annual Book of Standards–Section Four Construction, American Society for Testing Materials*, West Conshohocken, PA, USA, 2009.

[12] R. G. Kelly, J. R. Scully, D. W. Shoesmith, and R. G. Buchheit, "Electrochemical techniques in corrosion science and engineering," Maecel Dekker, Inc., New York, NY, USA, 2003.

[13] V. Feliu, J. A. Gonzalez, and S. Feliu, "Corrosion estimates from transient response to a potential step," *Corrosion Science*, vol. 49, no. 8, pp. 3241–3255, 2007.

[14] J. A. Gonzalez, J. M. Miranda, and S. Feliu, "Consideration on the reproducibility of potential and corrosion rate measurements in reinforced concrete," *Corrosion Science*, vol. 46, no. 10, pp. 2467–2485, 2004.

[15] K. N. Hoque and F. Presuel-Moreno, "Accelerated corrosion of steel rebar in concrete by electromigration: effect of reservoir length and concrete mixes," in *Proc. the 13th International Conference on Marine Technology (MARTEC 2022)*, 2023.

[16] K. N. Hoque and F. Presuel-Moreno, "Corrosion propagation of steel rebar embedded in marine structures prepared with binary blended concrete containing slag," in *Proc. the 13th International Conference on Marine Technology (MARTEC 2022)*, 2023.

[17] K. N. Hoque and F. Presuel-Moreno, "Corrosion behaviour of reinforcing steel embedded in fly ash concrete," in *Proc. the 13th International Conference on Marine Technology (MARTEC 2022)*, 2023.

[18] K. N. Hoque and F. Presuel-Moreno, "Corrosion of steel rebar embedded in ternary blended concrete exposed to high humidity environment," in *Proc. the 13th International Conference on Marine Technology (MARTEC 2022)*, 2023.

[19] K. Hoque, "Corrosion propagation of reinforcing steel embedded in binary and ternary concrete," *Ph.D. Dissertation*, Department of Ocean and Mechanical Engineering, Florida Atlantic University (FAU), Boca Raton, Florida, USA, 2020.

[20] F. Presuel-Moreno and K. Hoque, "Corrosion propagation of carbon steel rebar embedded in concrete," *Corrosion 2019*, Nashville, Tennessee, USA, 2019.

[21] F. Presuel-Moreno, K. Hoque, and A. Rosa-Pagan, "Corrosion propagation monitoring using galvanostatic pulse on reinforced concrete legacy samples," 2020-FAU-02 Final Report for National University Transportation Center TriDurLE, 2022.